5. Conclusions

The use of the CAD/CAM technique considerably speeds up the design work of a progressive tool. This is based on the CAD/CAM system's ability to unfold a 3D sheet part into a plane and the idea of using this geometry for all the process and tool design phases. Tool standard part libraries and stored expert data speed up the designing process further. However, the design and manufacture demand a considerable number of highly-skilled personnel and the effective use of the designer's skill and experience in designing metal-forming processes is still required.

Acknowledgment

References

1. Mattiasson, K. et al, Numerical Methods in Industrial Forming Processes. Balkema, Boston 1986.

2. Altan, T. et al, Metal Forming, Fundamentals and applications. Metals Park, Ohio 1986.

3. v. Finckenstein, E. & Kleiner, M., Process Simulation and Adaptive Controlling in Sheet Metal Forming. Advanced Technology of Plasticity, Berlin 1987 p. 1187-1194.

4. Stracke, J., Methodische Grundlagen für die rechnerunterstützte Bearbeitung von Anpassungskonstruktionen. Ruhr-Universität Bochum, Bochum 1980.

5. VDI Bildungswerk, Leistungssteigerung bei Werkzeugen der Stanztechnik. VDI, Düsseldorf 1987.

6. User's manual, Auto-trol CAD-system. Auto-trol Corporation, Denver 1986.

7. Seifert, H., Rechnerunterstütztes Konstruieren mit PROREN. Ruhr-Universität Bochum, Bochum 1986.

FINITE ELEMENT ANALYSIS OF SHEET METAL FORMING PROBLEMS USING A VISCOUS VOIDED SHELL FORMULATION

Eugenio Oñate
and
Carlos Agelet de Saracibar

Escuela Técnica Superior de Ingenieros de
Caminos, Canales y Puertos
Universidad Politécnica de Cataluña
08034 Barcelona, Spain

Summary

A formal analogy between the equations of pure plastic and viscoplastic flow theory for void containing metals and those of standard non linear elasticity is presented. It is shown how by direct simplifications of the general equations, the standard incompressible flow expressions for non voided metals are obtained. The general formulation is particularized for the analysis of sheet metal forming problems and details of the viscous voided shell and membrane formulations for dealing with the axisymmetric case are given. Finally, some examples of applications of pure and hemispherical stretching and deep drawing of a circular sheet are presented.

1. Introduction

It is well known that an effective way of treating the continuous deformation of metals is to use a rigid plastic flow model in which elastic effects are neglected. The simplest and perhaps most widely used model, uses the Von Mises yield criterion, which results in the incompressibility of the material flow. The governing equations in this case are entirely analogous to those of standard elasticity with a single material parameter, the shear modulus, playing the role of the non linear strain rate dependent viscosity, and the displacements and strains that of the velocities and strain rates in the analogous flow model respectively [1]. This analogy has allowed the solution of complex metal forming problems with standard finite element programs originaly written for 2D and 3D elasticity [2]-[4]. Applications of this approach in the context of sheet metal forming analysis leaded to the derivation of the so called *viscous shell model*. This is based on a simple modification of standard small displacement elastic shell theory using the mentioned flow-elasticity analogy [5].

163

Recently, Oñate *et al.* [6] have extended the viscous shell model to deal with *material degradation* effects by taking into account nucleation, growth and coalescence of microscopic voids in the deforming metal sheet. The resulting *viscous voided shell model* introduces the effect of material compressibility in the form of a two parameters constitutive model which can be simply identified as the equivalent shear modulus and Poisson's ratio of an analogous non linear elasticity material. This allows finite element solutions to be obtained for such potentially more difficult problems by directly using computer programs written for standard —compressible— elasticity.

The objective of this paper is to present in an unified form the basic concepts of the viscous shell model for plastic/viscoplastic materials including the effect of material degradation due to the development of microscopic voids, for the finite element analysis of sheet metal forming problems. The formulation will be particularized for the axisymmetric case using simple linear axisymmetric shell and membrane elements. Details of the treatment of the contact and friction effects are also briefly given. Finally, some examples of application of the general formulation to three examples of pure and hemispherical stretching and deep drawing of a circular sheet are presented.

2. Basic concepts

The basis of the plastic/viscoplastic flow approach is to neglect elastic stresses and strains in the deforming material [1],[3]. This assumption allows to write the following rate equation

$$\dot{\epsilon}_{ij} = \dot{\epsilon}_{ij}^{NL} = f(\sigma_{ij}) \tag{1}$$

where $\dot{\epsilon}_{ij}$ and $\dot{\epsilon}_{ij}^{NL}$ account for the total and non linear —plastic/viscoplastic— strain rate tensors, respectively. The form of function f depends on the type of plastic/viscoplastic constitutive model used. In any case (1) describes the behaviour of an equivalent *fluid* in which strain rates and velocities u_i are simply related by

$$\dot{\epsilon}_{ij} = \frac{1}{2}\left(\frac{\partial u_i}{\partial x_j} + \frac{\partial u_j}{\partial x_i}\right) \qquad \text{or} \qquad \dot{\epsilon} = Lu \tag{2}$$

and the stresses satisfy the standard equilibrium conditions [7]

$$\begin{aligned} L^T\sigma + b = 0 & \qquad \text{in the volume } V \\ M^T\sigma + t = 0 & \qquad \text{in the boundary } \Gamma \end{aligned} \tag{3}$$

where b and t are body force and surface load vectors, respectively, and M is a matrix containing the components of the unit normal to the boundary Γ.

In the following sections particular forms of (1) for different types of material behaviour will be presented.

2.1. RIGID PLASTIC FLOW OF VOID CONTAINING METALS

The yield condition for a randomly voided material with spherical —for 3D problems— or circular cylindrical voids —for plane stress problems— may be assumed following Gurson [8] as

$$\Phi = \frac{3}{2}\frac{s_{ij}s_{ij}}{\sigma_M^2} - \omega = 0 \tag{4}$$

where σ_{ij} and s_{ij} are the macroscopic Cauchy stress and stress deviator, respectively, σ_M is the tensile yield limit of the matrix material (assumed incompressible), f is the void volume fraction and

$$\omega = 1 - 2f\cosh\left(\frac{\sigma_{kk}}{2\sigma_M}\right) + f^2 \tag{5}$$

Note that for porosity parameter $f = 0$, $\omega = 1$ and (4) reduces to the classical Von Mises yield condition [2]. The change of the void volume fraction during the deformation increment is taken as [8]-[11]

$$\dot{f} = \dot{f}_g + \dot{f}_n + \dot{f}_c \tag{6}$$

where subscrits g, n and c stand for growth, nucleation and coalescence of voids. Also, it can be assumed that [9]-[10]

$$\dot{f}_g = (1-f)\dot{\epsilon}_{kk}^{(p)} \qquad \dot{f}_n = \frac{k}{\sigma_M}\left(\dot{\sigma}_M + \frac{\dot{\sigma}_{kk}}{3}\right) \tag{7}$$

the material parameter k being the volume fraction of particles converted to voids per unit fractional increase in stress. Nucleation is assumed to occur only if the approximate value of the maximum normal stress $\sigma_M + \frac{\sigma_{kk}}{3}$ exceeds in the current time increment its previous maximum. Finally, the term $\dot{f}_c$ can be numerically accounted for in the following way. According to [10], coalescence takes place at $f \simeq 0.2$. Thus a simple and effective numerical scheme can be used to reproduce this phenomenon if, at points for which $f = 0.2$, a proportional increase in f is assumed for a number of fixed incremental steps ($\simeq 5$), up to $f = 1$, for which the material carrying capacity in that point is effectively zero.

Using standard plasticity theory [8], it is possible to arrive at the following expression for the non linear —plastic— strain rates of eq. (1)

$$\dot{\epsilon}_{ij}^{(p)} = \dot{\epsilon}_{ij} = \frac{1}{2\bar{G}}\left(\sigma_{ij} - \frac{\bar{\nu}}{1+\bar{\nu}}\sigma_{kk}\delta_{ij}\right) \tag{8}$$

where

$$\bar{G} = \frac{\sigma_M}{3\bar{\epsilon}}\left(\frac{\omega + fAS}{1-f}\right) \tag{9}$$

$$\bar{\nu} = \frac{1-B}{2+B} \tag{10}$$

with $B = \frac{tS}{2A}$, $A = \frac{\sigma_{kk}}{2\sigma_M}$, $S = \sinh A$ and $\dot{\bar{\epsilon}} = \sqrt{\frac{2}{3}\dot{\epsilon}_{ij}\dot{\epsilon}_{ij}}$. After some manipulations a simpler expression for $\bar{G}$ can be found as

$$\bar{G} = \frac{\sigma_M \sqrt{\omega}}{3\sqrt{\dot{\bar{\epsilon}}^2 - \frac{2}{9}\dot{\epsilon}_{kk}^2}} \tag{11}$$

Comparing (8) with the constitutive equation for classical elasticity [7], and taking into account (2) and (3) it can be easily be concluded that *there is a perfect analogy between the equations of plastic flow of a voided metal and those of standard elasticity.*

Therefore, displacements and strains in the analogous elastic model, can be identified with the velocities and strain rates, respectively, and the elastic shear modulus and Poisson's ratio with parameters $\bar{G}$ and $\bar{\nu}$ given by (8)-(10). Note the stress/strain rate dependence of $\bar{G}$ and $\bar{\nu}$ which makes the analogous elastic problem non linear and the numerical solution must therefore be found iteratively.

2.2. PLASTIC FLOW OF NON VOIDED METALS

For *classical plastic materials* $f = 0$ and $\omega = 1$ and therefore, from (8)-(10) we have

$$\bar{\nu} = \frac{1}{2} \qquad \bar{G} = \frac{\sigma_M}{3\dot{\bar{\epsilon}}} \tag{12}$$

and

$$\dot{\epsilon}_{ij} = \frac{1}{2\bar{G}}\left(\sigma_{ij} - \frac{\sigma_{kk}}{3}\delta_{ij}\right) = \frac{s_{ij}}{2\bar{G}} \tag{13}$$

Thus the *incompressible* form of the deformation is recovered and the expression for the equivalent shear modulus $\bar{G}$ coincides with that of the non-Newtonian viscosity of the standard plastic flow problem [2].

2.3. INCLUSION OF VISCOPLASTIC EFFECTS

The expression for the viscoplastic strain rate can be postulated as [7]

$$\dot{\epsilon}_{ij} = \gamma\chi^n\frac{\partial\phi}{\partial\sigma_{ij}} \quad \text{for} \quad \chi > 0$$
$$\dot{\epsilon}_{ij} = 0 \quad\quad\quad \text{for} \quad \chi = 0 \tag{14}$$

where γ is the material fluidity and χ is the overstress parameter defined as

$$\chi = \sqrt{\frac{3}{2}\frac{s_{ij}s_{ij}}{\omega}} - \sigma_M \tag{15}$$

Note that for the non viscous case $\chi = 0$ (see eq. (4)).

Oñate *et al.* [6] have shown that accounting for the viscous properties of a

voided metal in the manner described above corresponds to replacing in (9) or (11) the matrix yield value σ_M by

$$\sigma_M\left[1 + \left(\frac{\dot{\bar{\epsilon}}}{\gamma\sigma_M^n\sqrt{\omega + 2\beta_1^2}}\right)^{\frac{1}{n}}\right] \tag{16}$$

with $\beta_1 = \frac{tS}{2}$. It is easy to see that for the particular case of non voided material ($f = 0, \omega = 1$) eqs. (9) and (16) lead to

$$\bar{G} = \frac{\sigma_M + (\frac{\dot{\epsilon}}{\gamma})^{\frac{1}{n}}}{3\dot{\bar{\epsilon}}} \tag{17}$$

which again exactly coincides with the expression of the fluid viscosity derived in [2].

3. Application to thin sheet metal forming problems

The analogy presented in previous sections allows the treatment of large plastic/viscoplastic deformations of thin sheets of metal making direct use of classical small displacement elastic shell theory. The solution scheme is thus as follows

1) Identify an elastic shell formulation. If standard finite element techniques [7] are used, a discrete system of equations is obtained, upon discretization, of the form

$$K(G, \nu)a = f \tag{18}$$

where K is the shell stiffness matrix and a and f are the displacement and nodal force vectors, respectively. The equivalent *viscous voided shell* is formulated by simply identifying displacements and strains with velocities and strain rates respectively, and the shear modulus and Poisson's ratio with parameters $\bar{G}$ and $\bar{\nu}$ given in previous section. For the simpler non voided case $\bar{\nu} = \frac{1}{2}$ and $\bar{G}$ is given by (12) or (17). Eq. (18) becomes a system of non linear equations which must be solved iteratively. In the initial solution values of velocities a^0, and void volume fraction f^0 must be specified.

2) Solve for a^1. If direct iteration is used the first iteration becomes

$$a^1 = [K(a^0)]^{-1}f \tag{19}$$

3) Check for convergence of velocities. If desired convergence is not achieved go back to 2.

4) Once convergence has been achieved the geometry is updated by $a\Delta t$, where Δt is an appropriate time step size, which can be taken as constant or equal to the time increment for which the first node of the non contacting region comes into contact with the indenting punch [5],[6]. Also, the boundary conditions must be changed if new points have come into contact with the tool surface. Finally, the values of the sheet thickness and void volume fraction are updated according to

the values of the thickness and volumetric strain respectively.

5) The process is restarted with the new values of the sheet geometry and void volume fraction.

The algorithm is thus very simple and it also allows other effects like strain hardening and friction conditions to be included in a straight-forward manner [6] (see also Section 5).

It is worth nothing that in well developed sheet forming stages the spatial velocity field does not change much between two consecutive solutions. Thus, significant savings in computer time can be obtained by updating the sheet geometry using the constant spatial velocity field for a number of incremental steps [6].

We have also to point out that direct iteration usually yields convergence of the velocity field after a small number of iterations. This is due to the well posed boundary value nature of the problem in which velocities are prescribed at the tool-blank contact nodes, and forces (reactions) are obtained 'a posteriori' from the converged velocity field. Thus for each solution the initial velocities can be guessed to be not too far from their correct values and convergence is rapidly achieved. Special care, however, must be taken to define the cut-off value of the equivalent shear modulus in zones of the sheet where rigid deformations are expected, to prevent ill conditioning of the stiffness matrix.

In the next sections we present details of the finite element viscous voided shell formulation for axisymmetric sheet metal forming problems.

4. Axisymmetric formulation

4.1. AXISYMMETRIC SHELL FORMULATION

The basis of the success of the *viscous shell* approach described in previous sections lies in the efficiency of the analogous elastic shell formulation. We will briefly present here the relevant expressions of the finite element axisymmetric formulation developed by Oñate *et al.* [5],[6] for thin sheet metal forming analysis. The formulation is based on Reissner-Mindlin shell theory and uses the simple two node linear element. Details of the shell theory can be found in [6],[13].

The velocity field, after discretization of the shell in axisymmetric linear elements, can be expressed as

$$\mathbf{u} = \left\{ \begin{array}{c} u \\ w \\ \theta \end{array} \right\} = \sum_{i=1}^{2} N_i a_i \quad \text{with} \quad N_i = N_i I_3 \quad \text{and} \quad a_i = \left\{ \begin{array}{c} u_i \\ w_i \\ \theta_i \end{array} \right\} \tag{20}$$

with u_i, w_i and θ_i being the two global velocities and the angular velocity of node i, respectively and N_i the linear shape function of node i. (*Figure 1*).
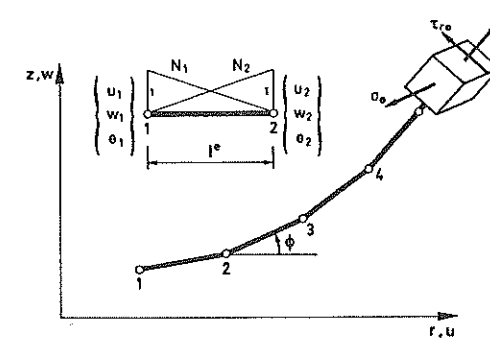
Figure 1.- Axisymmetric shell. Discretization in axisymmetric linear elements

The generalized strain rate and stress vectors can be expressed as

$$\dot{\epsilon} = [\dot{\epsilon}_r, \dot{\epsilon}_\theta, \dot{\gamma}]^T = \sum_{i=1}^{2} B_i a_i \tag{21}$$

$$\sigma = [\sigma_r, \sigma_\theta, \tau]^T = D\dot{\epsilon} = D \sum_{i=1}^{2} B_i a_i \tag{22}$$

where for an isotropic material

$$D = \begin{bmatrix} d_{11} & d_{12} & 0 \\ d_{21} & d_{22} & 0 \\ 0 & 0 & d_{33} \end{bmatrix} \tag{23}$$

with

$$d_{11} = d_{22} = 2\bar{G}\frac{1}{1-\bar{\nu}}, \qquad d_{12} = d_{21} = 2\bar{G}\frac{\bar{\nu}}{1-\bar{\nu}}, \qquad d_{33} = \bar{G} \tag{24}$$

where $\bar{G}$ and $\bar{\nu}$ are given by (9)-(11), and the expression of the strain rate matrix B_i is given in the Appendix.

The element contributions to the stiffness matrix K, and the nodal force vector f are

$$K_{ij}^{(e)} = 2\pi \int_{l^{(e)}} B_i^T \hat{D} B_j r ds \tag{25}$$

$$f_i^{(e)} = 2\pi \int_{l^{(e)}} N_i t r ds + 2\pi r_i p_i \tag{26}$$

where $l^{(e)}$ is the element length, r the radial distance, t and p, surface and point load vectors, respectively and the expression of matrix $\hat{D}$ is given in the Appendix. It has been shown that for a successfull use of this formulation the integral of (25) must be numerically computed using a single Gaussian integration point. This allows to obtain an explicit form of $K_{ij}^{(e)}$ as

$$K_{ij}^{(e)} = 2\pi \bar{B}_i^T \hat{D} \bar{B}_j \bar{r} l^{(e)} \tag{27}$$

where $(\tilde{\ })$ denotes values at the element midpoint. The expression of $\bar{B}_i$ is readily obtained by substituting the terms N_i and $\frac{\partial N_i}{\partial s}$ in eq. (A.1) by $\frac{1}{2}$ and $\frac{(-1)^i}{l(s)}$, respectively.

4.2. AXISYMMETRIC MEMBRANE FORMULATION

The membrane formulation can be easily derived from the general case presented in previous sections by simply neglecting in all expressions the flexural and shear terms. The relevant matrices and vectors are now defined as

Velocity field: $\qquad u = \left\{ \begin{array}{c} u \\ w \end{array} \right\} = \sum_{i=1}^{2} N_i I_2 a_i \qquad a_i = \left\{ \begin{array}{c} u_i \\ w_i \end{array} \right\}$ (28)

Generalized strain rate field: $\qquad \hat{\dot{\epsilon}} = \left\{ \begin{array}{c} \dot{\epsilon}_r \\ \dot{\epsilon}_\theta \end{array} \right\} = \sum_{i=1}^{2} B_{m_i} a_i$ (29)

Generalized stress field: $\qquad \hat{\sigma} = \left\{ \begin{array}{c} \hat{\sigma}_r \\ \hat{\sigma}_\theta \end{array} \right\} = D_m \hat{\dot{\epsilon}} = D_m \sum_{i=1}^{2} B_{m_i} a_i$ (30)

where

$$ D_m = t \begin{bmatrix} d_{11} & d_{12} \\ d_{21} & d_{22} \end{bmatrix} \qquad (31) $$

where t is the thickness, d_{ij} are given in (24) and

$$ B_{m_i} = \begin{bmatrix} \cos\phi \frac{\partial N_i}{\partial s} & \sin\phi \frac{\partial N_i}{\partial s} \\ \frac{N_i}{r} & 0 \end{bmatrix} \qquad (32) $$

Finally the explicit expression of the stiffness matrix for the linear element in this case is identical to (27) with B_{m_i} and D_m instead of B_i and $\hat{D}$, respectively.

5. Treatment of friction

An algorithm to simulate friction effects between the contact interfaces can be based on an simple adjustment of nodal reactions at contact nodes after each iterative solution, until they satisfy a Coulomb type of friction law. This method has been succesfully implemented by the authors [5],[6] and it is used in the examples presented in this paper.

A more consistent procedure to model contact and friction can be developed by imposing the contact conditions via a penalty type approach, using the total potential of the contact forces with the geometric compatibility conditions. Generally the contact constraints can be written as

$$ r = Ca - s \qquad (33) $$

where a is the velocity field at a particular deformed configuration and C and s are obtained from the appropiate sticking or sliding contact rule [14].

The expression of the total potential energy penalized using (33) is expressed as

$$ \Pi^* = \frac{1}{2} a^T K a - a^T f + \frac{1}{2} r^T \alpha r \qquad (34) $$

where α is a diagonal penalization matrix. The stationarity of (34) gives the modified system of equations to be solved at each iteration as

$$ [K + C^T \alpha C] a = f + C^T \alpha s \qquad (35) $$

The friction conditions can now be taken into account at each iteration by imposing a Coulomb type of relationship between the total resultant normal and tangential forces acting on each element belonging to the contact surface. This procedure is currently under development by the authors. For more general information see [14].

6. Examples

6.1. STUDY OF THE INFLUENCE OF POROSITY IN THICKNESS CHANGE

In the first example the effect of porosity development in the change of thickness in a circular sheet, of radius = 2.20 in. and an initial thickness of 0.035 in., under uniform stretching has been studied. The uniaxial stress–effective strain curve of the matrix material is given by

$$ \sigma_Y = 5.4 + 27.8\bar{\epsilon}^{0.504} \qquad \text{tn/in}^2 \qquad \bar{\epsilon} < 0.36 $$
$$ \sigma_Y = 5.4 + 24.4\bar{\epsilon}^{0.375} \leq 22.0 \qquad \text{tn/in}^2 \qquad \bar{\epsilon} \geq 0.36 $$

Fifty axisymmetric linear elements have been used in the analysis. The thickness strain and porosity distributions obtained for two cases with $k = 0.005$ and $k = 0.01$ respectively, in all the sheet and $f^0 = 0.0$ in all elements except $f^0 = 0.01$ in element 20 ($r \simeq 1.0$ in.) for both cases, are shown in *Figure 2*. It can be clearly seen in these figures that porosity development affects very strongly the otherwise uniform thickness strain field and causes strain localization as expected. Also from *Figure 2* it is clear that the inclusion of the void nucleation parameter k amplifies the mentioned localization effect.

6.2. HEMISPHERICAL STRETCHING OF CIRCULAR ISOTROPIC SHEET

The geometrical configuration of the problem is shown in *Figure 3*. Fifty axisymmetric linear elements have been used in the analysis. The uniaxial stress–effective strain curve of the matrix material is the same as in previous example. A friction coefficient of 0.04 has been used, as suggested in [15]. The problem has
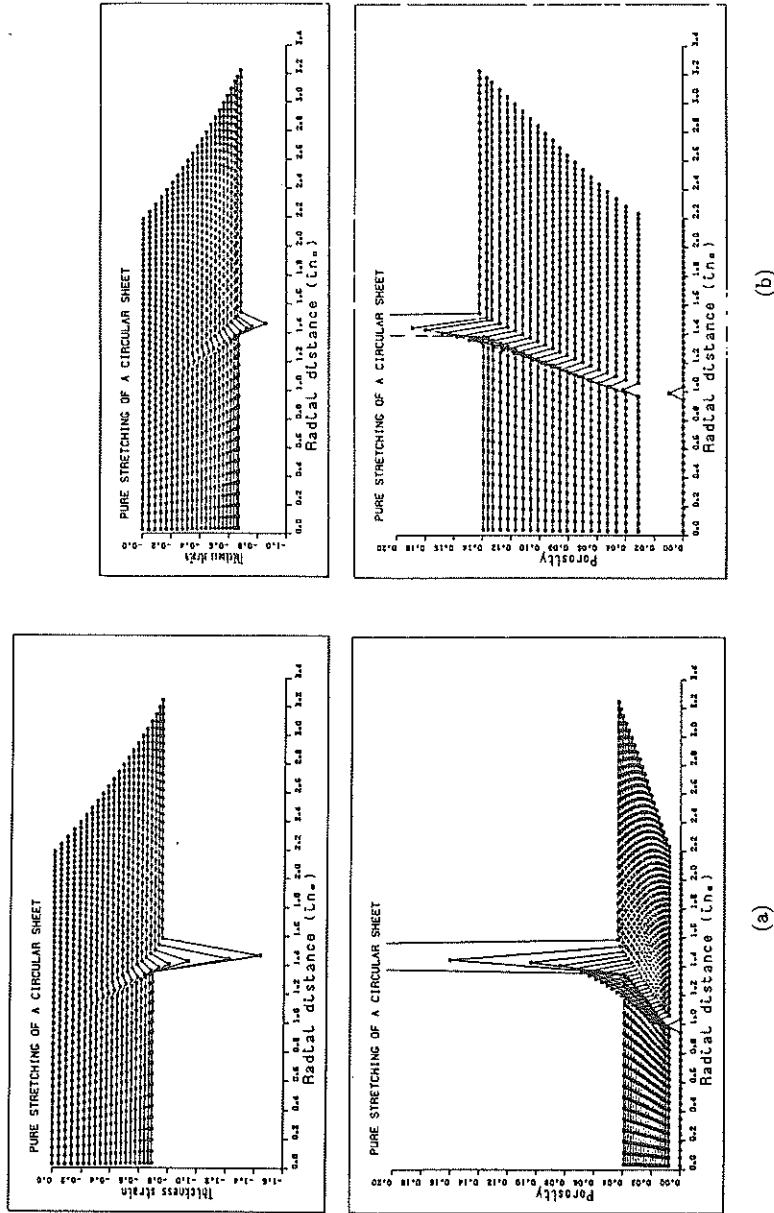
Figure 2.- Pure stretching of a circular sheet. Effect of porosity in thickness strain. $f^0 = 0$ in all the sheet except $f^0 = 0.01$ in element 20 ($r \simeq 1$ in.). (a) $k = 0.005$ (b) $k = 0.01$
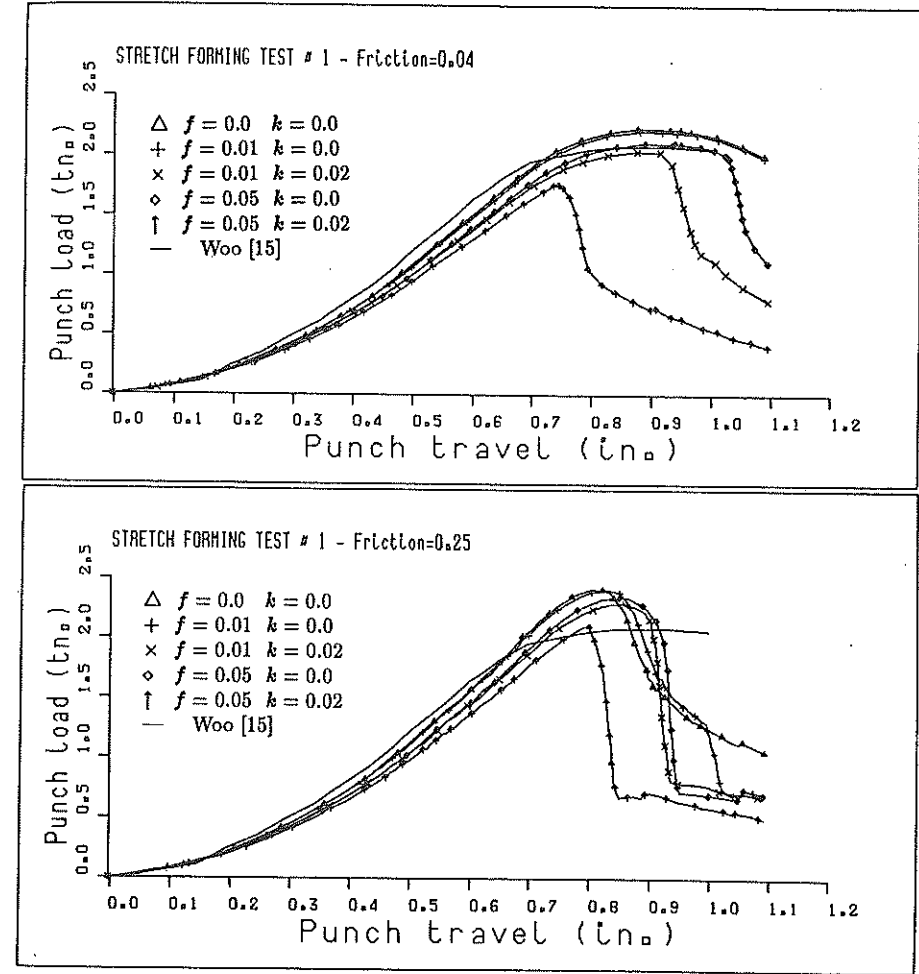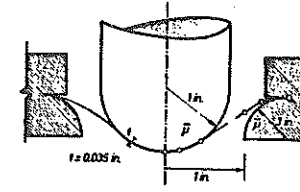
(a) (b)

Figure 3.- Hemispherical sheet forming.
Punch load-displacement curve for different porosity conditions.

been analysed for different initial void volume fractions of $f^0 = 0.0$, 0.01, and 0.05, and nucleation parameters $k = 0.0$ and 0.02 in all elements. Numerical results for the punch load–displacement curves for various values of f^0 and k are shown in Figure 3. From these results it can be deduced that:

(a) An increase of the initial void porosity and nucleation parameters causes a progressive reduction of the load carrying capacity of the sheet. Values of the maximum punch load obtained for $f^0 = 0.0$ and 0.01 with $k = 0.0$ and 0.02, and $f^0 = 0.05$ with $k = 0.0$, are in agreement with the experimental results reported in [15]. However, for $f^0 = 0.05$ and $k = 0.02$ a reduction of the maximum punch load of 35 per cent is obtained.

(b) Inclusion of void porosity induces localized failure with a rapid loss of rigidity which causes an almost vertical descent of the load–displacement curve.

6.3.   HEMISPHERICAL DEEP DRAWING OF CIRCULAR ISOTROPIC SHEET

The geometrical configuration of the problem is shown in Figure 4.   Fifty axisymmetric linear elements have been used for the analysis. The uniaxial stress–strain curve of the material is the same as in previous example.   A friction coefficient of 0.04 has been used [16].   Numerical results of the punch load–displacement curve and hoop and thickness strain distributions for $f = 0$ and $k = 0$ have been plotted in Figure 4.   Numerical results compare reasonably well with experimental ones [16]. Finally a 3D perspective of the sheet geometry at different deformation stages is shown in Figure 5.

7. Conclusions

The equations describing plastic and viscoplastic flow of metals including the effects of nucleation, growth and coalescence of voids, are analogous to those of classical non linear elasticity.   The formulation for non voided materials is directly obtained from the general case simply by neglecting the effect of voids, thus yielding the classical form analogous to incompressible elasticity. This allows standard finite element methods developed for elastic shell problems to be directly used for the analysis of complex sheet metal forming processes, including material degradation effects by development of microscopic voids.

The examples analysed show that by adjusting parameters such as the value and distribution of the initial void volume fraction and of the fraction of particles converted to voids per unit increase of stress, the model should be able to predict development of voids and localized material failure.

8. References

1. Zienkiewicz, O.C. and Godbole, P.N., 'Flow of plastic and viscoplastic solids with special reference to extrusion and forming processes', *Int. J. Num. Meth. Engng.*, 8, 3–16 (1979).
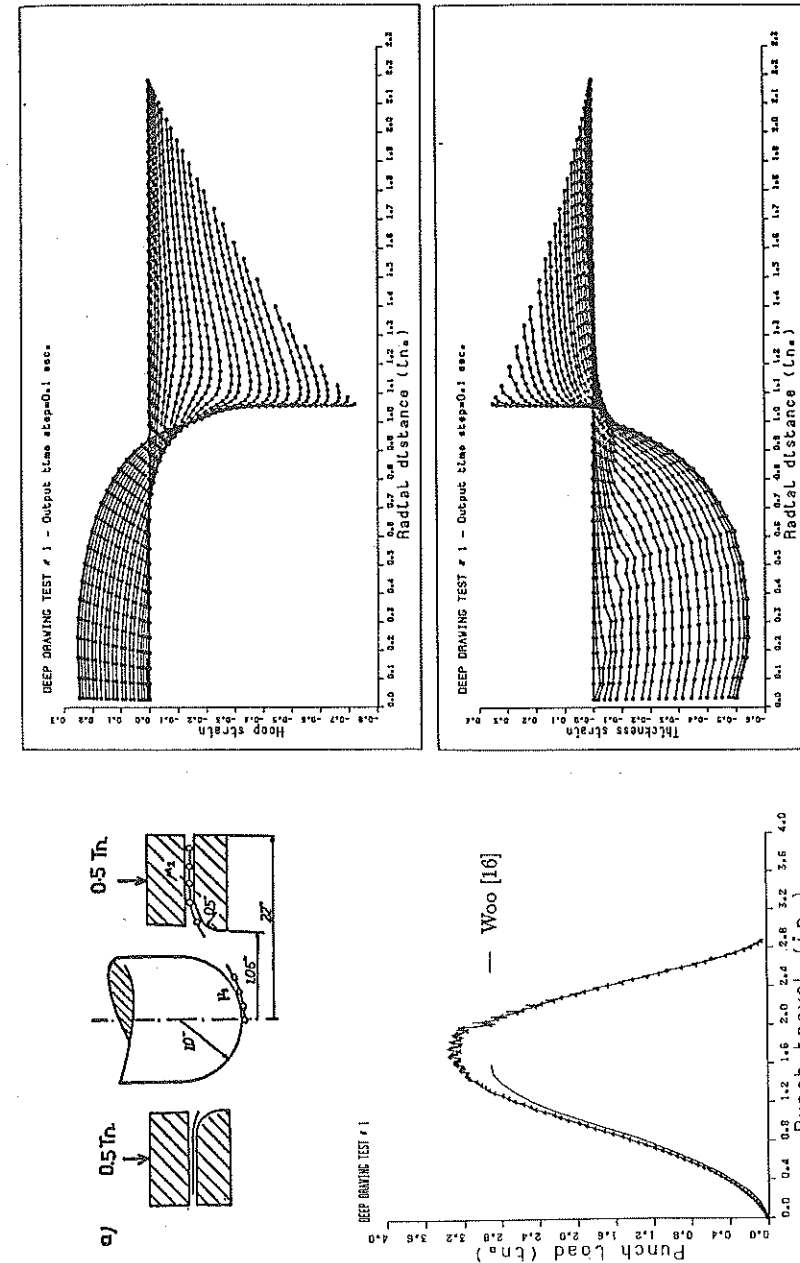
Figure 4.– Hemispherical deep drawing. (a) Punch load–displacement curves. (b) Hoop and thickness strain distributions for various deforming configurations.

(a) PT = 0.300 in.

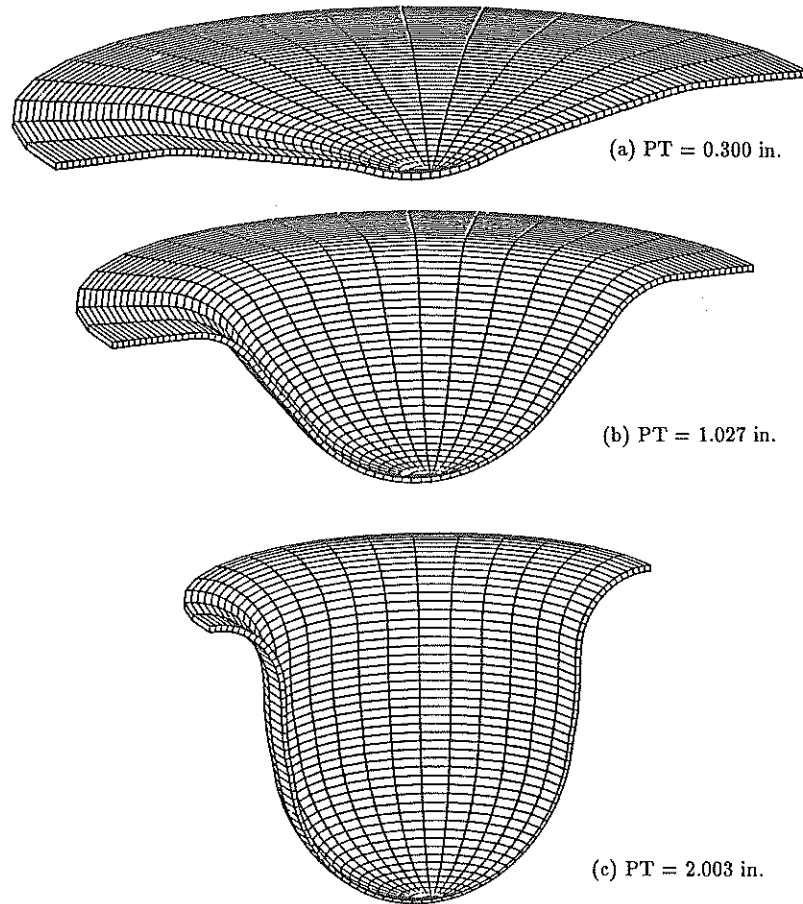(b) PT = 1.027 in.

(c) PT = 2.003 in.

Figure 5.- Hemispherical deep drawing.
Geometry of the sheet for various deforming configurations.
(PT = Punch travel)

2. Zienkiewicz, O.C., Jain, P.C. and Oñate, E., 'Flow of solids during forming and extrusion. Some aspects of numerical solutions', *Int. J. Solids Struct.,* **14**, 15–38 (1978).

3. Zienkiewicz, O.C., Oñate, E. and Heinrich, J.C., 'A general formulation for coupled thermal flow of metals using finite elements', *Int. J. Num. Meth. Engng.,* **17**, 1497–1514 (1981).

4. Pittman, J.F.T., Zienkiewicz, O.C., Wood, R.D. and Alexander, J.M. (eds.), *Numerical Analysis of Forming Processes*, Wiley, New York, 1984.

5. Oñate, E. and Zienkiewicz, O.C., 'A viscous shell formulation for the analysis of thin sheet metal forming', *Int. J. Mech. Sc.,* **25**, 305–335 (1983).

6. Oñate, E., Kleiber, M. and Agelet de Saracibar, C., 'Plastic and viscoplastic flow of void containing metals. Applications to axisymmetric sheet forming problems', *Int. J. Num. Meth. Engng.,* **25**, 225–251 (1988).

7. Zienkiewicz, O.C., *The Finite Element Method*, McGraw–Hill, 1979.

8. Gurson, A.L., 'Continuum theory of ductile rupture by void nucleation and growth. I. Yield criteria and flow rules for porous ductile media', *J. Eng. Mater. Tech.,* **99**, 2–15 (1977).

9. Needleman, A. and Rice, J.R., 'Limits to ductility set by plastic flow localization', *Mechanics of Sheet Metal Forming*. D.P. Koistinen and N.-M. Wang (eds.), 237–266, Plenum, N.Y., 1978.

10. Tvergaard, V., 'On localization in ductile materials containing spherical voids', *Int. J. Fracture,* **18**, 237–252 (1982).

11. Kleiber, M., 'Numerical study on necking-type bifurcations in void-containing elastic-plastic material', *Int. J. Solids Struct.,* **20**, 191–210 (1984).

12. Baynham, J.M.W. and Zienkiewicz, O.C., 'Developments in the finite element analysis of thin sheet drawing and direct redrawing processes using the rigid plastic approach', *Proceedings of International Conference on Numerical Methods in Industrial Forming Processes*, J.F.T. Pittman *et al.* (eds.), Pineridge Press, Swansea, 1982.

13. Zienkiewicz, O.C., Bauer, J., Morgan, K. and Oñate, E., 'A simple and efficient shell element for axisymmetric shells', *Int. J. Num. Meth. Engng.,* **11**, 1545–1559 (1977).

14. Bathe, K.J. and Chaudary, A., 'A solution method for planar and axisymmetric contact problems', *Int. J. Num. Meth. Engng.,* **21**, 65–88 (1985).

15. Woo, D.M., 'The stretch forming test', *The Engineer,* **220**, 876–889 (1965).

16. Woo, D.M., 'On the complete solution of the deep-drawing problem', *Int. J. Mech. Sci.,* **10**, 83–94 (1968)

Appendix

STRAIN RATE AND CONSTITUTIVE MATRIX FOR AXISYMMETRIC SHEET FORMULATION

Strain rate matrix
$$B = [B_1, B_2]$$

$$B_i = \begin{bmatrix} \cos\phi\frac{\partial N_i}{\partial s} & \sin\phi\frac{\partial N_i}{\partial s} & 0 \\ \frac{N_i}{r} & 0 & 0 \\ 0 & 0 & \frac{-\partial N_i}{\partial s} \\ 0 & 0 & -N_i\frac{\cos\phi}{r} \\ -\sin\phi\frac{\partial N_i}{\partial s} & \cos\phi\frac{\partial N_i}{\partial s} & -N_i \end{bmatrix} \qquad (A.1)$$

for definition of ϕ see *Figure 1*.

Constitutive matrix
$$\hat{D} = \int_{-\frac{t}{2}}^{\frac{t}{2}} S^T D S dz' \qquad (A.2)$$

$$S = \begin{bmatrix} 1 & 0 & z' & 0 & 0 \\ 0 & 1 & 0 & z' & 0 \\ 0 & 0 & 0 & 0 & 1 \end{bmatrix} \qquad D = \begin{bmatrix} d_{11} & d_{12} & 0 \\ d_{21} & d_{22} & 0 \\ 0 & 0 & d_{33} \end{bmatrix}$$

d_{ij} as given in (24). Note that the computation of $\hat{D}$ implies an integration across the thickness. This is in practice performed using numerical integration.

TIME STEPPING SCHEMES FOR THE NUMERICAL ANALYSIS OF SUPERPLASTIC FORMING OF THIN SHEET

J. BONET, R.D. WOOD and O.C. ZIENKIEWICZ
Civil Engineering Department, University College of Swansea, Swansea, SA2 8PP, Wales, U.K.

SUMMARY

The numerical simulation of the superplastic forming of thin sheet involves the time integration of velocities in order to determine the changing configuration of the sheet as it forms into the final component shape. During the course of developing a finite element analysis of the problem various time stepping schemes have been investigated. This paper discusses these schemes and reports on the success or otherwise of their implementation.

INTRODUCTION

Superplastic forming of products made from thin sheet is a manufacturing technique whereby, typically, titanium or aluminium alloy sheet, at sufficiently high temperature, can be blow formed, without fracturing, into a die to produce a very complex, light and strong component. In addition judicial use of the diffusion bonding characteristics of superplastic alloys enables assemblages to be formed which are structurally more integral than the same component produced by traditional means.

The crucial problem of predicting the relationship between the forming pressure cycle and the product thickness distribution can be ameliorated by using a finite element based numerical simulation of the forming behaviour, [1-8]. This usually involves a solution scheme in which velocities have to be integrated in order to ascertain the changing shape of the product as forming progresses. Furthermore, since the constitutive equations are nonlinear, the integration scheme is intimately connected to the nonlinear solution procedure.

This paper discusses explicit and implicit time stepping schemes associated with a finite element solution to the problem of simulating thin sheet superplastic forming. In particular, deficiencies experienced when the explicit scheme is used for general shapes are overcome by introducing a trapezoidal implicit scheme which is further improved by using a two step backward difference implicit scheme.